Microbiological Research 223–225 (2019) 22–32

Contents lists available at ScienceDirect

Microbiological Research

journal homepage: www.elsevier.com/locate/micres

Characterisation of ParB encoded on multipartite genome in *Deinococcus radiodurans* and their roles in radioresistance

Ganesh K Maurya[a,b], Swathi Kota[a,b], Hari S. Misra[a,b,*]

[a] Molecular Biology Division, Bhabha Atomic Research Centre, Mumbai, 400085, India
[b] Homi Bhabha National Institute, Mumbai, 400094, India

ARTICLE INFO

Keywords:
Centromere binding protein
Deinococcus
Genome segregation
Interdependence of genome maintenance and cell division
Multipartite genome system
Toroidal nucleoid
Radioresistance

ABSTRACT

The *Deinococcus radiodurans* multipartite genome consists of 2 chromosomes and 2 plasmids Its genome encodes 4 ParA and 4 ParB proteins on different replicons. Multiple sequence alignments of ParBs encoded on these genome elements showed that ParB of primary chromosome (ParB1) is close to chromosomal type ParB and is found to be different from ParBs encoded on chromosome II (ParB2) and megaplasmid (ParB3) elements. We observed that ParB1, ParB2 and ParB3 exist as dimer *in solution* and these proteins interact to self but not to its homologs in *D. radiodurans,* suggesting the specificity in ParBs dimerization. The *parB1* deletion mutant showed slow growth under normal condition and relatively reduced resistance to γ-radiation as compared to wild type. The *parB2* and *parB3* mutants maintained without selection pressure showed loss of radioresistance, which was not observed when maintained with selection pressure. Nearly half of the populations of these mutants showed resistance to antibiotics marked to respective genome elements. Interestingly, all the *parB* mutants showed increased copy numbers of cognate genome element in cells maintained with antibiotics possibly due to arrest in genome segregation. These results suggested that ParB proteins encoded on multipartite genome system in *D. radiodurans* form homodimer and not heterodimer with other ParB homologs, and they independently regulate the segregation of respective genome elements. The roles of ParB1 proteins in normal as well as radiation stressed growth of this bacterium have also been ascertained.

1. Introduction

The mechanisms underlying genome segregation are relatively better understood in eukaryotes where all three macromolecular events; chromosome duplication, segregation and cell division, are temporally separated (Yanagida, 2005). In bacteria, which have doubling time in minutes, these processes are not well separated but occur in same order like DNA duplication, segregation and cytokinesis and are believed to be interdependently regulated. Recently, genome sequencing studies have listed many bacteria that have multipartite genome system (MGS) comprised of more than one chromosome and large plasmids (Egan et al., 2005; Misra et al., 2018). Genome sequence analysis revealed that like bacteria harbouring monopartite genome, multipartite genome system harbouring bacteria also contain classical tripartite genome segregation (TGS) systems. TGS is comprised of *cis* elements termed bacterial centromere, Walker type P-Loop ATPases (ParA or ParA like proteins) and centromere binding proteins (ParB or ParB like proteins) (Hayes and Barilla, 2006; Gerdes et al., 2010). In brief, ParBs or its homologues show site specific interaction with centromeric sequences (usually present close to *parAB* operon in repeats) by HTH motif present in C-terminal region of protein. ParAs or its homologues are non-specific DNA binding ATPases which interact to *parB*-centromere segregation complex and undergo polymerisation / depolymerisation kinetics to segregates duplicated DNA. Different roles of Par proteins in bacterial survival have been reported in different bacteria. For instance, loss of chromosomal *parAB* locus is lethal and essential in *Caulobacter crescentus* (Mohl and Gober, 1997) but found to be dispensable in *Bacillus subtilis*, *Pseudomonas putida*, *Pseudomonas aeruginosa*, *Streptomyces coelicolor*, and *Vibrio cholerae* (chromosome I *parAB*) (Ireton et al., 1994; Lewis et al., 2002; Bartosik et al., 2004; Kim et al., 2000; Saint-Dic et al., 2006). Among multipartite genome system harbouring bacteria, the limited studies on genome maintenance have been reported in *V. cholerae* (Egan and Waldor, 2003; Fogel and Waldor, 2005), cystic fibrosis pathogen *B. cenocepacia* (Dubarry et al., 2006) and *D. radiodurans* (Charaka and Misra, 2012).

D. radiodurans is an extremotolerant bacteria characterized for its extraordinary resistance to DNA damaging agents including radiations and desiccation (Battista, 2000; Slade and Radman, 2011; Misra et al.,

* Corresponding author.
E-mail address: hsmisra@barc.gov.in (H.S. Misra).

https://doi.org/10.1016/j.micres.2019.03.005
Received 14 October 2018; Received in revised form 27 February 2019; Accepted 16 March 2019
Available online 01 April 2019
0944-5013/

2013). Multipartite genome of this bacterium consists of 2 chromosomes and 2 plasmids (White et al., 1999). Chromosome I, chromosome II and megaplasmid encode putative ParA and ParB proteins (White et al., 1999). Recently, chromosome I partitioning system has been characterized in *D. radiodurans* (Charaka and Misra, 2012). Involvement of ParA of chromosome II (ParA2) in the regulation of cell division has been reported (Charaka et al., 2013). Multiple sequence alignments of different ParA and ParB proteins encoded on multipartite genome elements in *D. radiodurans* showed close similarities with their homologs. Therefore, the importance of multiple sets of Par proteins with nearly similar putative structures and their possible functional redundancy in multipartite partite genome maintenance would be a curiosity to understand. Molecular mechanisms underlying the evolution and maintenance of multipartite genome system, its inheritance into daughter cells, and their functional significance in extreme phenotypes of *D. radiodurans* are not known in detail and would be worth studying.

Here, we report characterization of ParB proteins *in vitro* and their roles in extraordinary phenotypes in *D. radiodurans*. We demonstrated that all the ParBs form homodimer *in vitro* and do not interact with other ParB homologues of this bacterium. The *ΔparB2, ΔparB3* mutants maintained with antibiotic pressure showed nearly wild type growth under normal and γ-radiation stressed conditions. However, when maintained without selection pressure, a significant population was found to be sensitive to antibiotics and these cells compromised to γ-radiation resistance. This indicated that certain population in respective mutant has failed to receive copy of genome element marked with antibiotic resistance. The *ΔparB1* cells showed growth retardation under normal conditions and were sensitive to γ-radiation as compared wild type cells. All the mutants grown under selection pressure showed a significant increase in copy number of respective genome elements. Interaction of ParBs with replication initiation proteins DnaA and DnaB implied a functional interaction of genome duplication and segregation in this bacterium. These results together suggested that ParBs form homodimer and have roles in interdependent regulation of DNA replication and genome segregation as well as in radioresistance in *D. radiodurans*.

2. Materials and methods

2.1. Bacterial strains, plasmids and materials

All the bacterial strain and plasmids used in this study have been listed in Table S1 while primers in table S2. *D. radiodurans* R1 (ATCC13939) was a kind gift from Professor J. Ortner, Germany (Schaefer et al., 2000). It was grown in TGY (Tryptone (1%), Glucose (0.1%) and Yeast extract (0.5%)) medium at 32 °C. *E. coli* strain Nova Blue was used for cloning and maintenance of all the plasmids. *E. coli* strain BL21 (DE3) pLysS was used for the expression of recombinant proteins. *E. coli* strain BTH 101 was used for Bacterial Two-Hybrid System (BACTH) based study. *E. coli* cells harbouring pET28a (+) and its derivatives were maintained in the presence of kanamycin (25 μg/ml). Standard protocols for all recombinant techniques were used as described in (Green and Sambrook, 2012). All the molecular biology grade chemicals and enzymes were purchased from Sigma Chemicals Company, USA, Roche Biochemicals, Mannheim, Germany, New England Biolabs, USA and Merk India Pvt. Ltd. India.

2.2. Bioinformatic analysis

Multiple sequence alignment and functional motifs search in ParB1 (Dr_0012), ParB2 (DR_A0002), ParB3 (DR_B0002) and ParB4 (Dr_B0030) proteins were carried out using standard online bioinformatics tools as described earlier (Das and Misra, 2011; Charaka et al., 2013). In brief, the amino acid sequences of ParB1, ParB2, ParB3 and ParB4 proteins were subjected to a PSI-BLAST search with the SWISSPROT database. After five iterations, the sequences obtained were aligned by CLUSTAL-W along with ParB (Spo0J) protein of closest bacteria *T. thermophilus* and *B. subtilis*. The sequences of close homology were aligned by T-COFFEE, and the conserved motifs were marked in CLUSTAL-W. The secondary structure was inferred from PSIPRED, JNET, and Prof with the Quick2D server of the Max Planck Institute for Developmental Biology. The boundaries of the secondary structure (correspond to Spo0J of *T. thermophilus* (PDB. ID: 1VZ0)) were defined by using online Espript program. The secondary structure of C-terminal region was analyzed by using Psipred online software and represented in Espript online software. The phylogenetic tree between deinococcal ParBs and known ParB family proteins (Spo0J from *T. thermophilus* and *B. subtilis*) was constructed using PHYLIP program showing Neighbour-joining tree without distance corrections.

2.3. Cloning, expression and purification of ParB1, ParB2 and ParB3 proteins

Details of the primers used for construction of recombinant plasmids and generation of deletion mutants are given in Table S2. Genomic DNA of D. radiodurans R1 was prepared as reported previously (Battista et al., 2001), and open reading frames (ORFs) DR_A0002 (parB2) and DR_B0002 (parB3) were PCR amplified from genomic DNA by using primers pETB2F and pETB2R for the parB2 gene and primers pETB3F and pETB3R for the parB3 gene (see Table S2). PCR products were ligated at the NdeI and XhoI sites in pET28a (+) to yield pETB2 and pETB3, respectively. For ParB1, pET0012 plasmid (Charaka and Misra, 2012) was used. These plasmids were used for protein purification. Recombinant ParB1, ParB2 and ParB3 were expressed on pET0012, pETB2 and pETB3 respectively in E. coli BL21 (DE3) pLysS. The recombinant proteins were purified by nickel affinity chromatography, as described earlier (Charaka and Misra, 2012). In brief, overnight grown cultures of E. coli BL21 (DE3) pLysS expressing recombinant proteins were diluted 1:100 in fresh LB broth containing 25 μg/ml kanamycin and 0.5 mM isopropyl-β-D-thiogalactopyranoside (IPTG) was added at 0.3 OD at 600 nm and after 2 h culture was kept at 4 °C for overnight. It was further allowed to grow at 37 °C for 1 h and harvested to keep cell pellet in −70 °C. Cell pellet was thawed and suspended in buffer A (20 mM Tris–HCl, pH 7.6, 300 mM NaCl and 10% glycerol) containing 10 mM imidazole, 0.5 mg/ml lysozyme, 1 mM PMSF, 1 mM $MgCl_2$, 0.05% NP-40, 0.05% TritonX-100, protease inhibitor cocktail) and incubated at 37 °C for 30 min. Cells were sonicated for 5 min at 10 s pulses with intermittent cooling for 15 s at 25% amplitude. The cell lysate was centrifuged at 11,000 rpm for 30 min at 4 °C. The supernatant was dialysed in Buffer A containing 1 mM PMSF at 4 °C. The dialysed cell-free extract was loaded onto $NiCl_2$ charged-fast-flow-chelating-sepharose column (GE Healthcare) pre-equilibrated with buffer A containing 10 mM imidazole. The column was washed with 40 column volumes of buffer A containing 50 mM imidazole and 10 column volumes of buffer A containing 70 mM imidazole till proteins stop coming from the column. Recombinant proteins eluted in steps using 100 mM, 200 mM, 250 mM and 300 mM imidazole in buffer A and analyzed on 10% SDS-PAGE. Fractions containing more than 95% pure protein were pooled and dialyzed in buffer A containing 100 mM NaCl and processed for ion exchange chromatography using HiTrap Q HP anion exchange column (GE Healthcare Life sciences). Different fractions were analyzed on SDS-PAGE and fractions containing pure protein were pooled and concentrated using 10 kDa cut-off spin columns. Concentrated protein was centrifuged at 16,000 rpm for 30 min to remove aggregates. Supernatant containing mostly soluble proteins were used for size exclusion chromatography. For storage in −20 °C, proteins were dialyzed in dialysis buffer containing 20 mM Tris-HCl pH 7.6, 100 mM NaCl, 50% glycerol, 1 mM $MgCl_2$ and 1 mM PMSF. Protein concentration was determined by taking OD at 280 nm in Nano drop (Synergy H1, Hybrid Multi-Mode Reader Biotek) using mass extinction co-efficient of the proteins.

Table 1
Copy number of different replicons in wild type (WT) and *parB* mutants with and without expression of respective ParBs *in trans* in *Deinococcus radiodurans*. Two genes per replicon (one near to origin and other near to terminus) were selected and copy number values have been tabulated accordingly.

	Chromosome I		Chromosome II		Megaplasmid		Small Plasmid	
Pheno -type	*ftsZ* 87°	*ftsE* 212°	*pprA* 334°	Dr_A0155 137°	Dr_B0003 6°	Dr_B0076 187°	DrC0001 0.55°	DrC0018 145°
WT	8.03 ± 0.33	7.28 ± 0.3	5.95 ± 0.35	5.55 ± 0.32	10.85 ± 0.32	10.06 ± 0.22	9.12 ± 0.26	8.69 ± 0.24
ΔB1	10.3 ± 0.11	9.62 ± 0.10	6.5 ± 0.16	6.01 ± 0.15	11.86 ± 0.13	11.02 ± 0.12	10.22 ± 0.09	9.59 ± 0.08
ΔB1/B1	7.85 ± 0.39	7.22 ± 0.32	6.2 ± 0.34	5.85 ± 0.31	10.96 ± 0.24	10.23 ± 0.18	8.96 ± 0.25	8.29 ± 0.23
ΔB2	8.89 ± 0.3	7.86 ± 0.27	9.55 ± 0.31	8.89 ± 0.28	13.08 ± 0.29	12.55 ± 0.38	11.22 ± 0.13	10.79 ± 0.12
ΔB2/B2	8.25 ± 0.13	7.88 ± 0.11	6.15 ± 0.13	5.88 ± 0.12	11.12 ± 0.12	10.59 ± 0.21	9.34 ± 0.18	8.9 ± 0.17
ΔB3	8.78 ± 0.24	8.02 ± 0.21	7.86 ± 0.24	7.12 ± 0.22	18.25 ± 0.33	17.55 ± 0.45	12.24 ± 0.38	11.52 ± 0.36
ΔB3/B3	8.31 ± 0.32	7.62 ± 0.29	6.02 ± 0.41	5.78 ± 0.37	11.45 ± 0.35	10.81 ± 0.25	9.15 ± 0.31	8.78 ± 0.29

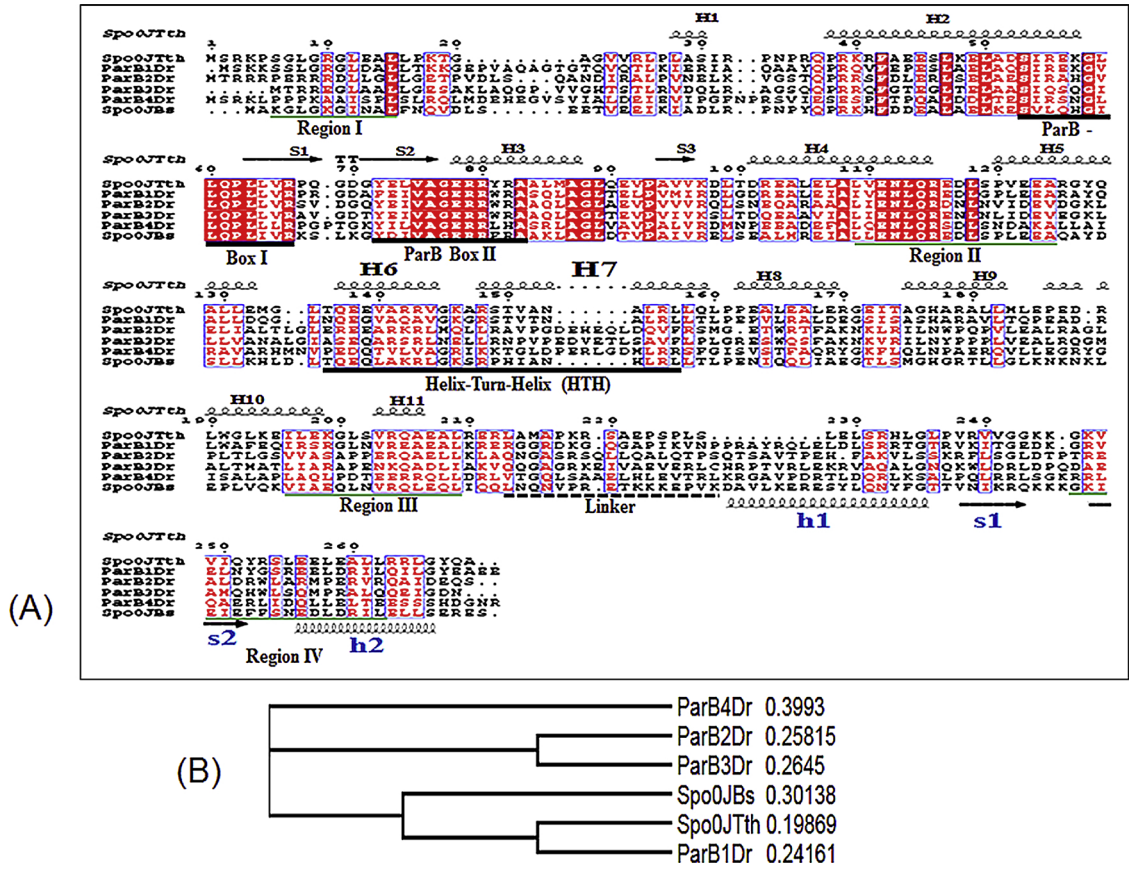

Fig. 1. Multiple sequence alignment of deinococcal ParB proteins with known ParB family proteins. The amino acid sequence of different deinococcal ParB proteins, Spo0J from *B. subtilis* and *T. thermophilus* is retrieved from NCBI and homology between sequences is checked by ClustalW analysis. Boundaries of the secondary structure were defined using online Espript program. The secondary structure shown in this figure corresponds to those of domain of Spo0J of *T. thermophilus* (PDB. ID: 1VZ0). Secondary structure of C-terminal region was analyzed by using Psipred online software and represented in Espript online software (A). The phylogenetic tree between deinococcal ParBs and known ParB family proteins was constructed using PHYLIP program showing Neighbour-joining tree without distance corrections (B).

2.4. Size exclusion chromatography and glutaraldehyde crosslinking

For determination of the molecular weight of deinococcal ParB proteins in its native state, molecular size exclusion chromatography was performed using Superdex™ 200 G L column (Pharmacia) on AKTA purifier (GE Healthcare). For this, ˜1 mg of purified ParB1, ParB2 and ParB3 proteins were loaded separately onto the column in storage buffer containing 20 mM Tris HCl, 100 mM NaCl, pH 7.6 and eluted at a flow rate of 0.5 ml/min. The column was formerly calibrated with gel filtration molecular weight markers (Amersham-Pharmacia: Chymotripsinogen- 25 kDa, Ovalbumin- 44 kDa, Bovine serum albumin – 66.5 kDa, Aldolase – 158 kDa, Catalase- 250 kDa). Standard calibration curve was plotted with elution volume of marker against the logarithm of molecular weight of markers. The molecular weight of the purified ParBs in the native condition was determined by fitting the elution volume into the calibration curve. Eluted peaks were analyzed on native PAGE for reconfirmation of the presence of ParB proteins (data not shown).

For glutaraldehyde crosslinking of protein in their native state, ˜10 µg of the purified recombinants ParB1, ParB2 and ParB3 proteins were diluted in 20 mM phosphate buffer pH 8.0 in a reaction volume of 30 µl. Further, protein solutions were incubated at 37 °C for 5 min in absence and presence of 2 µl of freshly prepared 0.02% glutaraldehyde solution. To this, equal volume of 2X cracking dye was added and

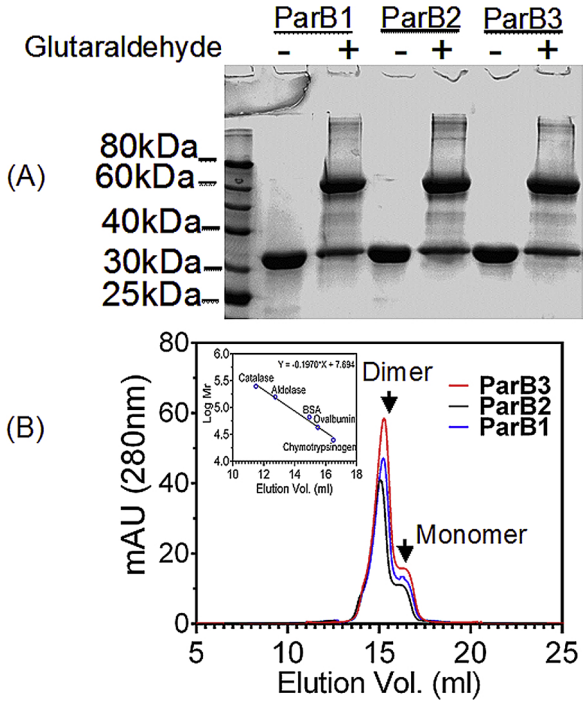

Fig. 2. Molecular size / weight determination of recombinant ParB1, ParB2 and ParB3 proteins in solution using glutaraldehyde crosslinking (A) and size exclusion chromatography (B). In brief, ~10 µg of the purified recombinants ParB1, ParB2 and ParB3 proteins were incubated in 20 mM phosphate buffer pH 8.0 in the absence and presence of 0.02% glutaraldehyde solution at 37 °C for 5 min. The reaction mixture was heated at 80 °C in presence of 2X cracking dye and separated on 10% SDS-PAGE and stained with Coomassie brilliant blue (A). For size exclusion chromatography, ~1 mg of purified ParB1, ParB2 and ParB3 proteins were passed through Superdex™ 200 G L column (Pharmacia) on AKTA purifier (GE Healthcare) at a flow rate of 0.5 ml/min. The column was formerly calibrated with gel filtration molecular weight markers and standard calibration curve was plotted with elution volume of marker against the logarithm of molecular weight of markers (given in inset of Fig. 2B). The molecular weight of the purified ParBs in the native condition was determined from standard curve (B). The given data is representative of experiments repeated three times independently.

heated at 80 °C for 5 min. These samples were separated on 10% SDS-PAGE and stained with Coomassie brilliant blue and documented.

2.5. *In vivo* protein-protein interaction studies in *D. radiodurans*

Interaction among ParB1, ParB2 and ParB3 was monitored in *D. radiodurans* by co-immunoprecipitation. For that, the T18 tagged *parB*s were PCR amplified using BTHF(pv) and BTHR(pv) primers from their BACTH derivative plasmids (Maurya et al., 2016) and cloned in pVHS559 plasmid (Charaka and Misra, 2012) at *Nde*I-*Xho*I sites to yield pV18B1, pV18B2 and pV18B3 (Table S1). Similarly, N-terminal hexahistidine tagged *parB, parB2* and *parB3* were amplified using pETHisF and pETHisR primers from their pET28a + derivatives (Table S1) and cloned in pRADgro plasmid (Misra et al., 2006) at *Apa*I-*Xba*I sites to yield pRADhisB1, pRADhisB2 and pRADhisB3 plasmids (Table S1). The expression of fusion proteins in *Deinococcus* from these constructs was monitored using Anti-T18 antibodies or Anti-polyhistidine antibodies (Maurya et al., 2018) (Fig. S2 A, B). The deinococcal cells co-expressing T18 tagged ParBs with hexahistidine tagged ParBs in different combinations were collected at log phase. The cell-free extracts of *D. radiodurans* expressing all three ParBs under IPTG induction as on pV18B1, pV18B2 and pV18B3 in different combinations with hexahistidine tagged all three ParBs under constitutive promoter from pRADgro were prepared and immunoprecipitated using Anti-polyhistidine antibodies as described earlier (Maurya et al., 2016, 2018). The T18 fused or polyhistidine fused ParBs alone were used as controls. The immunoprecipitates were separated on SDS-PAGE, blotted onto PVDF membrane and hybridized using monoclonal antibodies against T18 tag. The hybridization signals were detected using anti-mouse secondary antibodies conjugated with alkaline phosphatase using BCIP/NBT substrates (Roche Biochemical, Mannheim). The interaction between replication initiator protein, DnaA and deinococcal ParBs in *D. radiodurans* was monitored by using co-immunoprecipitation. In brief, N-terminal hexahistidine tagged dnaA (DR_0002) was PCR amplified using pETHisF and pETHisR primers from pETDnaA plasmid (dnaA cloned in pET28a + at *Bam*HI and *Eco*RI sites) and cloned in pRADgro plasmid at *Apa*I and *Xba*I sites. The resulting plasmid named as pRADhisdnaA. The expression of hexahistidine tagged DnaA in *D. radiodurans* from pRADhisdnaA was monitored through western blotting by using Anti-polyhistidine antibody as described above (Fig. S2 C). The pRADhisdnaA was co-transformed with T18 tagged deinococcal ParBs expressing plasmid as mentioned above. The expression of T18

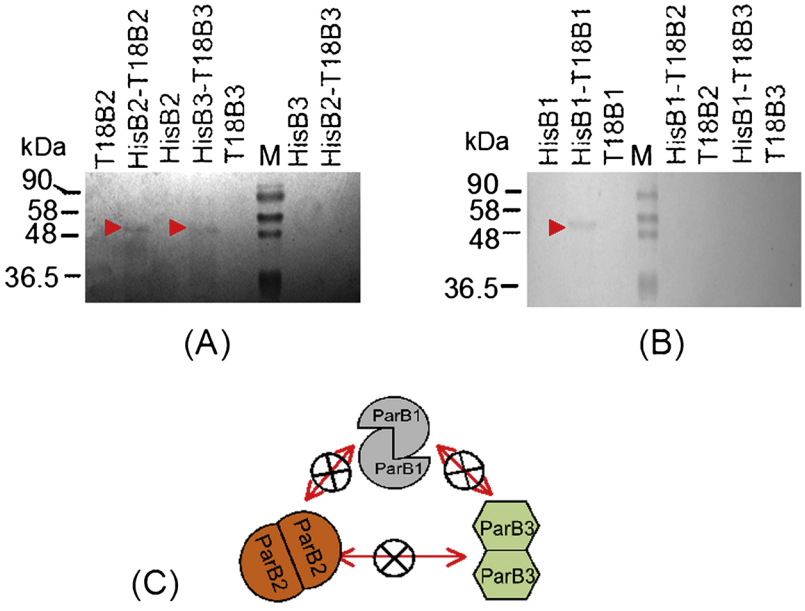

Fig. 3. *In vivo* interaction among deinococcal ParBs from *D. radiodurans* using co-immunoprecipitations. Plasmid bearing polyhis tagged ParB1 (HisB1), ParB2 (HisB2) or ParB3 (HisB3) were co-transformed with plasmid bearing T18 tagged ParB1 (T18B1), ParB2 (T18B2) or ParB3 (T18B3) in different combinations (see table S1). For controls these constructs were co-transformed along with empty vectors. These transformants were grown and induced with required amount of IPTG (see methods). The cell lysate of equal O.D. co-transformants were used for co-immunoprecipitation using polyhistideine antibodies. Equal amount of co-IPs was separated on SDS-PAGE and immunoblotted using T18 antibodies (Fig. 3A–B). Data in panel A and B are the representatives of a reproducible experiment repeated 3 times. Based on these observations from *D. radiodurans,* a cartoon model has been made to show interactions among deinococcal ParBs (C).

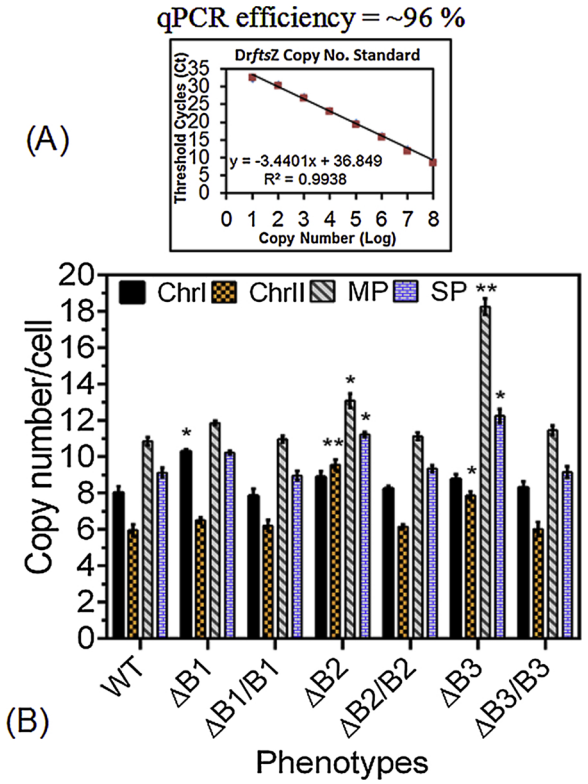

Fig. 4. Effect of *parB1, parB2* and *parB3* mutation on the ploidy of deinococcal genome. The wild type (WT) cells, *parB1 (ΔB1), parB2 (ΔB2)* and *parB3 (ΔB3)* mutants and its complemented forms (*ΔB1/B1, ΔB2/B2* and *ΔB3/B3* respectively) were subjected to copy number determination for each replicon using quantitative Real Time PCR (qRT-PCR) as detailed in method. In brief, a fragment of about 300 bps of *DrftsZ* gene was PCR amplified and their know concentration was used for generating standard curve for copy number determination using qRT-PCR (A). Two different genes per replicon with similar PCR efficiency (> 96%) was selected in *D. radiodurans* (described in methods; Table 1). The qRT-PCR was carried out and the cycle threshold (Ct) values were determined. The replicon copy number is quantified by comparing the Ct values with standard (B). Average of copy number reflected from two genes per replicon was represented as mean ± SD (B). The student *t*-test was used for statistical analysis of obtained data. The P values, obtained at 95% confidence intervals, are shown as (*) for < 0.05, (**) for < 0.01 and (***) for < 0.001. The data is representative of experiments repeated three times.

tagged ParBs in co-transformants was induced by 5 mM IPTG. The cell-free extracts of *D. radiodurans* expressing all three ParBs as on pV18B1, pV18B2 and pV18B3 in different combinations with hexahistidine tagged DnaA under constitutive promoter from pRADgro were prepared and immunoprecipitated using Anti-polyhistidine antibodies as mentioned above (Maurya et al., 2016, 2018). The T18 fused ParBs or polyhistidine fused DnaA alone were used as controls. The co-immunoprecipitates were separated on SDS-PAGE, blotted onto PVDF membrane and hybridized by Anti-T18 monoclonal antibodies raised in mouse. The hybridization signals were detected as described above.

2.6. Protein-protein interaction study using BACTH system in surrogate E. coli

For protein-protein interaction studies between deinococcal ParBs and replication initiation protein DnaA as well as replication helicase DnaB, coding sequences of Dr_0002 (DnaA) and Dr_0549 (DnaB) were cloned at *Bam*HI-*Eco*RI sites and *Kpn*I-*Eco*RI sites in pKNT25 to yield pKNTDA and pKNTDB, respectively while pUTCB1, pUTCB2 and pUTCB3 was used as described in (Maurya et al., 2016) (Table S1). The expression of T25 tagged DnaA and DnaB in *E. coli* was monitored using Anti-T25 antibodies (Fig. S2 D). *In vivo* interactions of different proteins were monitored using bacterial two-hybrid system (BACTH) as described earlier (Karimova et al., 1998; Maurya et al., 2016). In brief, BTH101 was co-transformed with pKNTDA or pKNTDB in different combination with pUTCB1, pUTCB2 and pUTCB3 plasmids expressing target proteins with T25 or T18 tags. Empty vector pUT18 co-transformed with pKNTDA was used as negative controls while pUTEFA and pKNTEFZ were co-transformed as positive control. The co-transformants were spotted on LB agar plate containing 5′ bromo 4 chloro-3-indolyl-β-D-galactopyranoside (X-Gal) (40 μg/mL), IPTG (0.5 mM) and antibiotics as required and the appearance of white-blue color colonies was recorded. Further, β-galactosidase activity of same combinations was measured from liquid cultures and calculated in Miller units as described in (Battesti and Bouveret, 2012; Maurya et al., 2016) and plotted with standard deviation in GraphPad Prizm5.

In addition, co-immunoprecipitation was performed for *in vivo* interaction of deinococcal ParBs with DnaB in surrogate *E. coli.* Briefly, cell lysates of *E. coli* BTH 101 cells co-expressing different ParBs (ParB1, ParB2 and ParB3) with T18 tag from BACTH plasmids (table S2) in combination with DnaB from pKNTDB were immunoprecipitated using Anti-T25 antibodies as described in (Maurya et al., 2016). The immunoprecipitates were separated in 10% SDS-PAGE and blotted on PVDF membrane. The membrane was hybridized with Anti-T18 monoclonal antibodies and the hybridization signals were detected calorimetrically as described above.

2.7. Construction of parB deletion mutants in D. radiodurans

The parB1 deletion mutant of D. radiodurans was used as described in (Charaka and Misra, 2012). For generation of parB2 and parB3 deletion mutant of D. radiodurans, suicide plasmids pNOKA02 and pNOKB02 respectively were constructed from pNOKOUT (Khairnar et al., 2008) by using a strategy described previously (Charaka and Misra, 2012). In brief, the fragments 1 kb upstream and 1 kb downstream of ORFs Dr_A0002 and Dr_B0002 were PCR amplified with primers (see Table S2) and cloned at the *Kpn*I-*Eco*RI and *Bam*HI-*Sac*I sites in pNOKOUT plasmid, respectively. The recombinant plasmid thus obtained pNOKA02 and pNOKB02, was linearized with *Xmn*I and transformed into D. radiodurans cells. Transformants were maintained through several rounds of sub-culturing, and the homozygous replacement of parB2 and parB3 with nptII was ascertained by PCR amplification using internal primers of both genes (Fig S1). For complementation of deletion mutants, pV18B1, pV18B2 and pV18B3 plasmids (Table S1) were used which express trans copy of proteins under IPTG induction. These plasmids were transformed in respective mutants with vector control. The recombinant clones were scored on TGY plates in the presence of kanamycin (8 mg/ml) and spectinomycin (70 mg/ml). The deletion mutants and its complemented forms were used for subsequent studies.

2.8. Cell survival studies

Deinococcus radiodurans wild type cells, its *parB* mutants and complemented forms were subjected to 6 kGy γ-radiations as described in (Misra et al., 2006). In brief, the bacteria grown in TGY medium with and without appropriate antibiotics (kanamycin; 8 mg/ml) at 32 °C were washed and suspended in sterile phosphate-buffered saline (PBS) and treated with 6 kGy γ-radiation at dose rate 1.81 kGy/h (Gamma Cell 5000, ^{60}Co, Board of Radiation and Isotopes Technology, DAE, India). Irradiated cells with SHAM controls were washed in PBS and suspended in the fresh TGY medium. Equal numbers of cells were grown in 48 well microtiter plates (Nunclon; Sigma-Aldrich) containing TGY medium in presence and absence of required antibiotics or 5 mM IPTG (for induction ParBs from plasmid during complementation). Growth was monitored in replicates at 32 °C for 18 h using Synergy H1 Hybrid multi-mode microplate reader. In addition, growth rate was

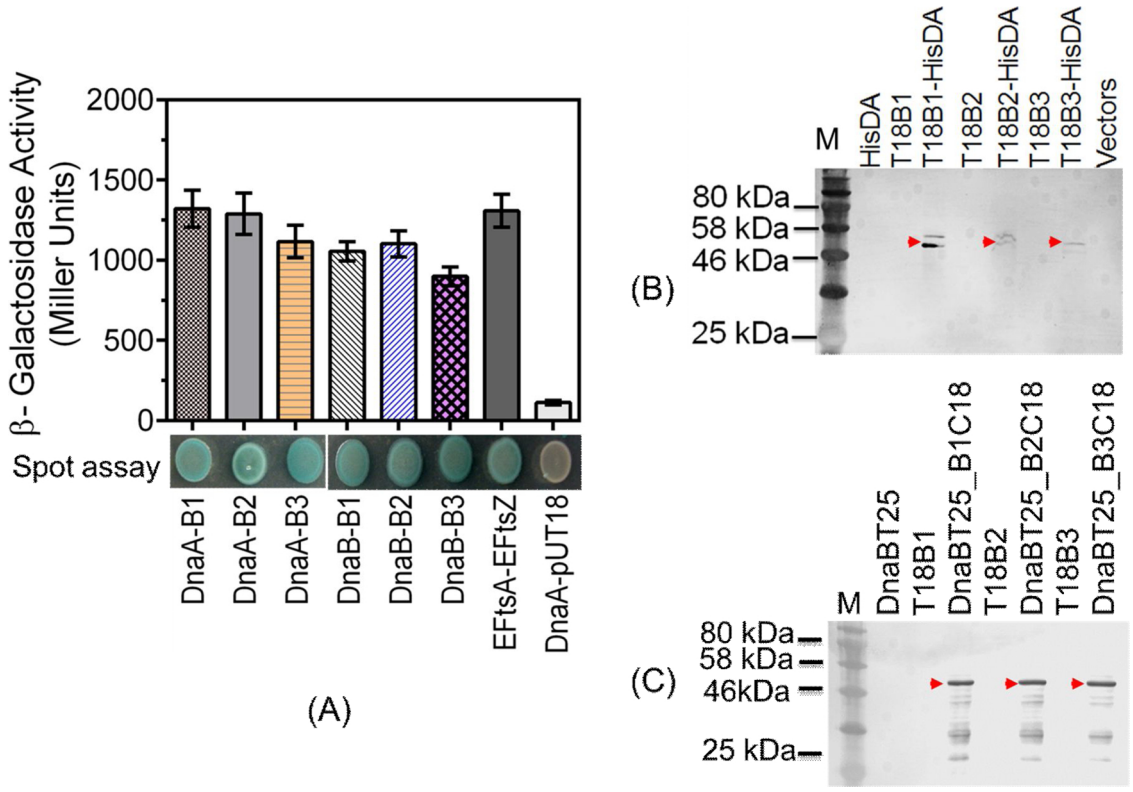

Fig. 5. Interaction of deinococcal ParBs with replication initiation protein DnaA and DnaB helicase. In brief, DnaA and DnaB from pKNT25 (as DnaA or DnaB) and deinococcal ParBs from pUT18C (as B1, B2 and B3) was co-expressed in BTH 101 strain of *E. coli*. Here *E. coli* FtsA from pKNT25 (EFtsA) and FtsZ from pUT18 (EFtsZ) was used as a positive control while DnaA with pUT18 empty vector was used as negative control. The obtained colonies were subjected to blue-green colonies spot and β-galactosidase assay (as described in methods) (A). For interaction of deinococcal ParBs with DnaA in *Deinococcus*, polyhis tagged DnaA (HisDA) from pRADhisDnaA was co-expressed with T18 tagged ParBs (as T18B1, T18B2 and T18B3 from pV18B1, pV18B2 and pV18B3 respectively) in different combinations in *D. radiodurans*. The cell lysate of co-transformants expressing the target proteins were imunoprecipitated by using polyhistidine antibody. The imunoprecipitates were separated on 10% SDS-PAGE and immunoblotted using T18 antibodies (B). For DnaB and ParBs interaction study from *E. coli* using co-IP, E. coli BTH101 cells co-expressing DnaB from pKNT25 (as DnaBT25) and ParBs from pUT18C (as B1C18, B2C18 and B3C18) in different combinations were lysed and immunoprecipitated using Anti-T25 antibody. The imunoprecipitates were separated on 10% SDS-PAGE and immunoblotted using T18 antibodies (C). Data in panel A is representative of reproducible experiment repeated 3 times while in panel B and C are repeated 2 times independently.

calculated for each sample type by following formula ($Nt = N0 * (1 + r)^t$); where Nt is OD_{600} at time t, N0 is OD_{600} at the start of growth curve, r is growth rate and t is time passed. For gamma radiation dose response studies, the wild type cells and different *parB* mutants were grown in absence and presence of kanamycin (antibiotic selection) and treated with different doses (0–8 kGy) of γ-radiations at dose rate of 1.81 kGy/h as described in (Misra et al., 2006). The irradiated cells with their SHAM control were washed in PBS and serially diluted. Different dilution from both the conditions (- / + kanamycin) were plated on TYG agar in absence and presence of kanamycin. The colony forming units (CFU) were recorded after 36–40 h of incubation at 32 °C. The survival fractions are expressed as a percentage of the number of colonies obtained with respect to untreated cells. Additionally, D_{10} value was determined for each sample from the survival curve and plotted.

2.9. Cell disruption and ploidy determination in mutants/complemented forms using quantitative real-time PCR

The mutants as well as their complemented cells of similar O.D. at 600 nm were harvested from appropriate growth condition by centrifugation. The cell number in all was determined using a Neubauer cell counter. The cells were washed with 70% ethanol solution and resuspended in a lysis solution containing 10 mM Tris pH 7.6, 1 mM EDTA and 4 mg/ml lysozyme and were incubated at 37 °C for complete cell lysis, the cell debris was removed by centrifugation (10,000 rpm, 5 min). Lytic efficiency was verified by the densities with a Neubauer counting chamber. The integrity of genomic DNA was confirmed by agarose gel electrophoresis. The aliquots of the cytoplasmic extract were serially diluted and 0.1 ml of it was used as for further analysis of genomic copy number using quantitative Real-Time PCR as described in (Breuert et al., 2006). In brief, a fragment of about 300 bps was amplified using standard PCRs with isolated genomic DNA from *D. radiodurans* R1 (ATCC13939) as a template. It was purified by Gel Extraction kit (Qiagen, Inc) and the amount of DNA was quantified by nanodrop, and the concentration was calculated using the molecular mass computed with 'oligo calc' (www.basic.northwestern.edu/biotools). A dilution was generated for each standard fragment and used for qPCR standardization. Two genes per replicon with similar PCR efficiency were selected in *D. radiodurans viz. ftsE* (212° position) and *ftsZ* (87° position) of chromosome I, Dr_A0155 (137° position) and *pprA* (334° position) of chromosome II, Dr_B0003 (6° position) and Dr_B0076 (187° position) of megaplasmid and Dr_C0001 (0.55° position) and Dr_C0018 (145° position) of small plasmid (Table 1, Table S2). PCR efficiency of each gene for amplification of internal 300 bps fragments was ascertained and was found to > 96% for each (data not shown). The qPCR was carried out by following the MIQE (minimum information for publication of quantitative real-time PCR experiments) guidelines using Roche Light cycler (Bustin et al., 2009) and optimum cycle threshold (Ct) values. Three independent biological replicates were used for each sample. The replicon copy number is quantified by comparing the results with a dilution series of a PCR product of known concentration

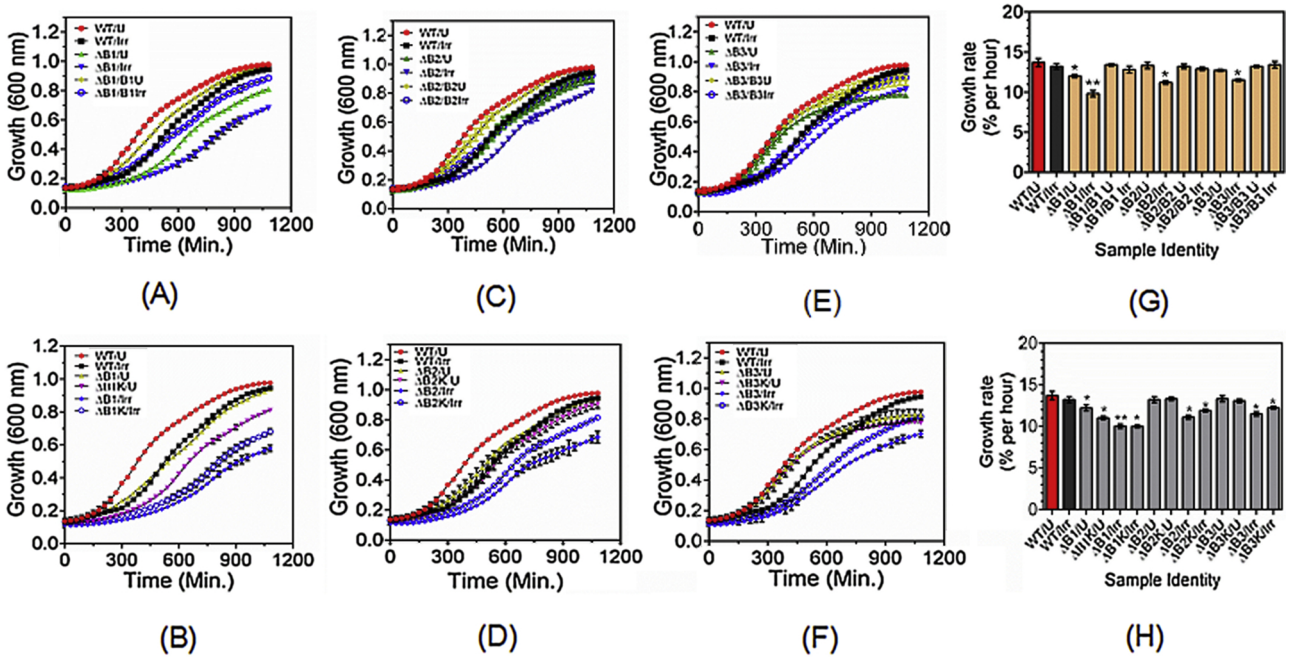

Fig. 6. Survival of *parB1, parB2* and *parB3* mutants to gamma radiation stresses. In brief, wild type (WT) cells, *parB1 (ΔB1), parB2 (ΔB2)* and *parB3 (ΔB3)* mutants and its complemented forms (*ΔB1/B1, ΔB2/B2* and *ΔB3/B3* respectively) were grown in required antibiotics (kanamycin; 8 μg/ml) and treated with 6kGy γ-radiation at dose rate 1.81 kGy/h. Irradiated cells (Irr) with SHAM controls (U; Unirradiated cells) were washed in PBS and suspended in fresh TGY medium. Equal numbers of cells were grown in 48 well microtiter plates containing TGY medium along with required antibiotics at 32 °C for 18 h and their growth was monitored at 600 nm wavelength using microplate reader. The growth curve of *ΔB1* and its complementation (A) *ΔB2* and its complementation (C) as well as *ΔB3* and its complementation (E) is representative of experiments repeated three times in triplicates and shown here as mean ± SEM (n = 9). In addition, wild type (WT) cells, *parB1 (ΔB1), parB2 (ΔB2)* and *parB3 (ΔB3)* mutants were grown in absence of kanamycin and treated with 6kGy γ-radiation. Equal numbers of irradiated cells with SHAM controls were grown in TGY medium in absence and presence of kanamycin (denoted as K; 8 μg/ml) at 32 °C for 18 h and their growth was monitored at 600 nm wavelength using microplate reader. The growth curve of *ΔB1* (B) *ΔB2* (D) as well as *ΔB3* (F) is representative of experiments repeated three times in triplicates and shown here as mean ± SEM (n = 9). The growth rate for each sample in Fig. 6(A–C) as well as (D–F) was calculated using formula ($Nt = N0 * (1 + r)^t$) and plotted in figure G & H, respectively. Statistical analysis was performed on this using 'student *t*-test'. The P values obtained at 95% confidence intervals are shown as (*) for < 0.05, (**) for < 0.01 and (***) for < 0.001.

that is used as a standard. The copy number of each replicon by both genes per cell was calculated using the cell number present at the time of cell lysis. Average copy number reflected from two genes per replicon was represented with appropriate bio-statistical analysis.

3. Results

3.1. Comparison of ParBs of D. radiodurans with ParB family proteins

Multiple sequence alignment of ParB proteins encoded on chromosome I (ParB1); chromosome II (ParB2) and megaplasmid (ParB3 and ParB4) with ParB homologs showed that ParB1 had an overall homology with the Spo0J of *T. thermophilus* and ˜40–60% identity with other chromosomal ParB proteins (Fig. 1A). Secondary genome ParBs like ParB2, ParB3 and ParB4 had only ˜30% identity amongst themselves and grossly different from the chromosomal type ParB's. Secondary structure prediction of all 4 ParBs using Spo0J structure template (PDB ID: 1VZ0) (Leonard et al., 2004) showed a characteristic HTH motif formed by helices H6 and H7 and remaining helices help in compaction of the domain (Fig. 1A). Further, phylogenetic analysis revealed that secondary genome ParBs form separate clade from primary genome ParB (Fig. 1B) (Dubarry et al., 2006). Except ParB1, the remaining ParBs have an extra sequence in the Helix-Turn-Helix (HTH) region. This might provide flexibility to these ParBs for their interaction with yet uncharacterized centromeric sequences on their cognate genome elements. These proteins also showed different C-terminal region as compared to Spo0J, which might provide specific interaction of these ParB with their cognate ParA during segregation process.

3.2. ParBs of D. radiodurans dimerises in solution

Since, ParBs in other bacteria are known to function as dimers, dimerization of purified ParB1, ParB2 and ParB3 was checked using glutaraldehyde cross-linking and size-exclusion chromatography approaches. Results showed that a large proportion of total proteins in all ParBs exist as dimer *in solution* (Fig. 2). For instance, majority of ParB showed a molecular size of ˜ 60 kDa on SDS-PAGE after cross-linking (Fig. 2A) and these proteins were eluted at the same volume where of BSA (˜66.5 kDa) eluted in size-exclusion chromatography (Fig. 2B). *In vivo* oligomeric nature of ParB proteins was checked by immunoprecipitation. For that different ParBs were tagged with either T18 in pVHS559 or polyhis in pRADgro plasmids and co-expressed in different combinations in *D. radiodurans*. Expression of these fusion products of ParBs was monitored by immunobloting (Fig. S2A, S2B). The total proteins from log phase cells were immunoprecipitated using polyhis antibody, and the perspective interacting partners duly tagged with T18 was detected using T18 antibodies. All ParBs showed homotypic interactions indicating a possibility of homodimerization in *D. radiodurans*. None of them showed heterotypic interactions with other ParBs indicating less possibility of cross talk between different ParBs in this multipartite genome harbouring bacteria (Fig. 3A–C). These results corroborated earlier finding where full-length Spo0J of *T. thermophilus* was shown to exist in a dimer *in solution*. The roles of C-terminal region in Spo0J of *T. thermophilus* (Leonard et al., 2004) and in ParB of *Pseudomonas aeruginosa* (Bartosik et al., 2004) has been shown in dimerization and these dimers are required for binding to cognate centromeric sequences. These results suggested that ParBs encoded on different genome elements in *D. radiodurans* are less likely to interact with each other.

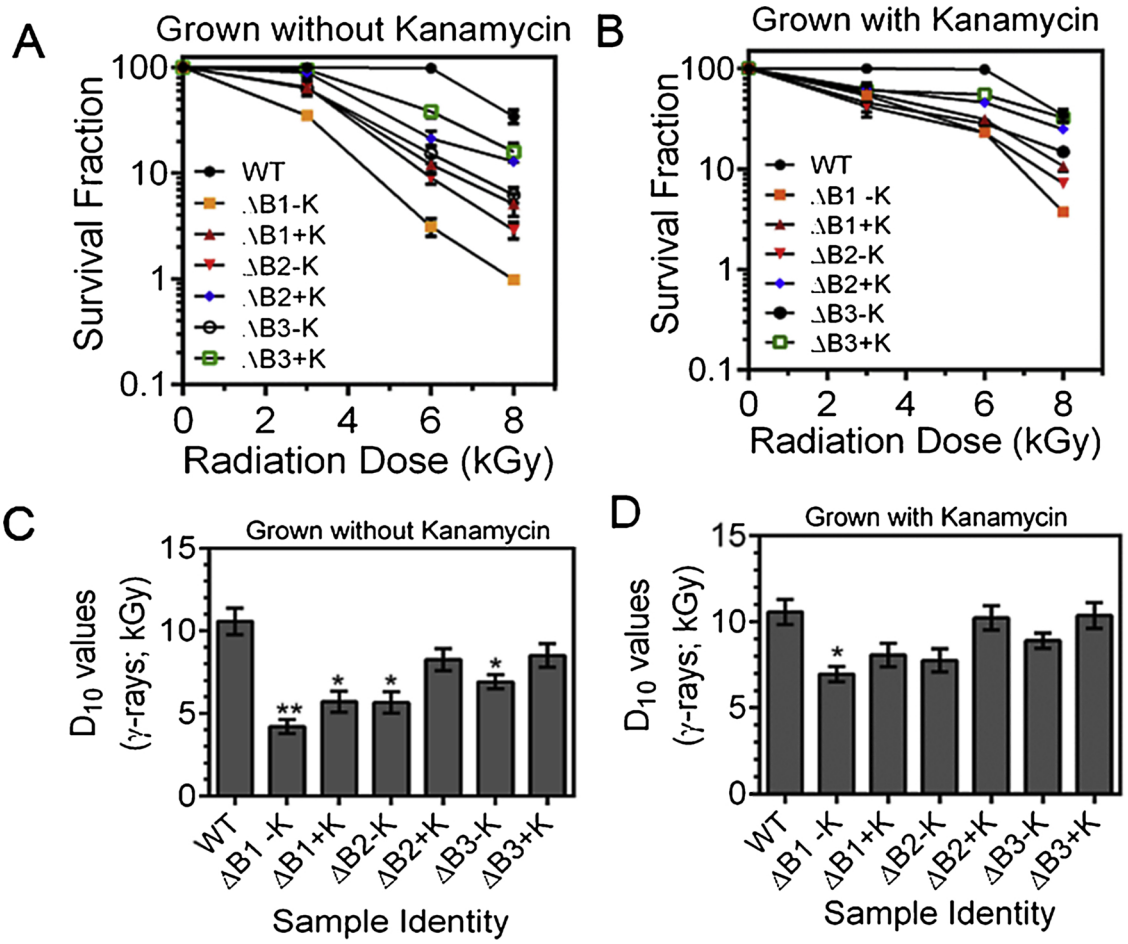

Fig. 7. Gamma radiation response of *parB* mutants of *D. radiodurans* grown with and without selection pressure. The deletion mutant of *parB1* (ΔB1), *parB2* (ΔB2) and *parB3* (ΔB3) were grown in absence (A) and presence (B) of kanamycin in TYG broth. The wild type (WT) and mutant cells were exposed to different doses of gamma radiation. Different dilution of irradiated cells as well as their SHAM controls were plated on TYG agar with (+K) and without kanamycin (-K). The survival fraction of each mutant with respect to radiation dose and antibiotics was compared with survival of unirradiated cells and plotted. The given data is representative of experiment repeated twice independently. The D10 values plot (C, D) was generated from survival curve A & B respectively. Statistical analysis was performed on this using 'student *t*-test'. The P values obtained at 95% confidence intervals are shown as (*) for < 0.05, (**) for < 0.01 and (***) for < 0.001.

3.3. Mutation in parB1, parB2 or parB3 has affected ploidy of cognate genome element

D. radiodurans harbours 8–10 haploid genome copies during exponential growth phase (Hansen, 1978; Harsojo and Matsuyama, 1981). Since, *parB* proteins are integral part of genome segregation in dividing population, the possibility of *parB* deletions affecting the copy number of daughter cells was examined. We monitored copy number of each replicons using quantitative real time PCR as described in methods. We used two genes per replicon (one near origin and other near terminus) and listed the values of copy number per gene per replicon in Table 1. Surprisingly, the copy number of cognate replicons had increased in respective null mutant of deinococcal *parB*s grown in the presence of required selection pressure. For instance, in Δ*parB1* the copy number of chromosome I has increased from 8–10, Δ*parB2* showed chromosome II copy number increase from 6 to 10 and the copy number of megaplasmid was increased from 11 to 18 in *parB3* mutant (Fig. 4). A marginal increase in the copy number of genome elements which was less than 2 times is intriguing and could not be explained merely by arrest of genome segregation. Earlier, the regulation of DNA replication by genome segregation events has been reported in *B. subtilis* where an increased genomic content was reported upon deletion of *parB* homolog (*spo0J*) in this bacterium (Lee et al., 2003, 2006). To be more specific with the involvement of ParBs in copy number variations, the functional complementation by *in trans* expression of these proteins in respective mutants was carried out. Results showed the resumption of original copy number near to wild type, which could suggest that deinococcal ParBs play the important roles in the regulation of replication initiation by yet uncharacterized mechanisms, in *D. radiodurans*.

3.4. ParBs interact with replication initiation proteins of D. radiodurans

Since, ploidy increase in *parB* mutant was less than 2-fold it indicated a strong possibility of arrest of replication progression in the absence of DNA segregation leading a marginal increase in DNA content. Thus, a possible cross talk between genome segregation and DNA replication was hypothesized. The *D. radiodurans* genome encodes replication initiation proteins DnaA and DnaB while *E. coli* homolog of DnaC is missing (White et al., 1999). This might suspect the functional redundancy of DnaC with some other proteins of this bacterium. We monitored *in vivo* interaction of ParB1, ParB2 and ParB3 with DnaA and DnaB using Bacterial Two Hybrid System (BACTH) in surrogate *E. coli* (Karimova et al., 1998; Maurya et al., 2016) as well as using co-immunoprecipitation from *D. radiodurans* (Maurya et al., 2018). The *E. coli* (*cyaA*$^-$) cells co-expressing DnaA / DnaB with all three deinococcal ParBs in different combinations on BACTH plasmids were screened for resumption of CyaA regulated expression of β-galactosidase activity. This was monitored by spot assay as well as *in solution* as described in methods. Results show that both DnaA and DnaB interacted with all three ParBs with nearly same levels as evident from the intensity of blue

colour colonies in spot assay as well as β-galactosidase activity levels *in solution* (Fig. 5A). In addition, co-immunoprecipitation assay of total soluble proteins of *D. radiodurans* cells co-expressing polyhis tagged DnaA in different combination with T18 tagged ParBs completely supported BACTH findings (Fig. 5B). Likewise, the co-immunoprecipitation assay from *E. coli* (*cyaA*$^-$) cells co-expressing DnaB on pKNTDB and ParB1, ParB2 or ParB3 on pUTCB1, pUTCB2 or pUTCB3, respectively in different combinations agreed with BACTH findings (Fig. 5C). This suggested that replication proteins can interact with all three ParBs encoded on multipartite genome of *D. radiodurans*. The similar observation was reported earlier in *V. cholerae,* where genome segregation proteins (ParA and ParB) were found interacting with DnaA (Kadoya et al., 2011). Our results suggested a cross-talk between DNA replication and segregation components of *D. radiodurans* and a strong possibility of interdependent regulation of these macromolecular events at least in this bacterium.

3.5. Secondary genome elements contribute in radioresistance

ParB is key protein that regulates the partitioning of duplicated genome elements into daughter cells in bacteria, and the null mutants of *parBs* in *D. radiodurans* showed increased copy number of genes estimated in different genome elements. This can be explained on the assumption that genome duplication would have occurred normally at least one round, but genome segregation, which maintains constant copy number per cell, got arrested and led to an increase in copy number under selection pressure. If this assumption is true, then cell density of mutants maintained in the presence and absence of selection pressure should be different. To test it, these cells were grown in the presence and absence of antibiotics and then growth kinetics were monitored under normal and gamma radiation stressed conditions. We observed that Δ*parB1* mutant maintained with or without selection pressure showed nearly similar trends of gamma radiation effects on its growth (Fig. 6A, B, G & H) suggesting the role of primary chromosome in growth irrespective of selection pressure. However, when Δ*parB2* and Δ*parB3* mutants were maintained in the presence or absence of selection pressure, they showed differential growth response under normal and radiation stressed conditions. For instance, the cells maintained under selection pressure showed nearly wild type effects of gamma radiation on their growth (Fig. 6C, D, G & H). When these were maintained in the absence of selection pressure, they showed a significant growth retardation under radiation stressed conditions as compared to that maintained with selection pressure (Fig. 6E–H). These results might suggest that Δ*parB2* and Δ*parB3* deletion does not affect normal growth of this bacterium while Δ*parB1* does, and the cell population that does not show resistance to antibiotic seems to be the one that is devoid of genome element(s) having replacement of cognate *parB* with antibiotic resistance marker gene. Logically, such population could have arisen when segregation of genome elements having *parB* replaced with antibiotic marker cassette does not occur, and that would support the role of ParBs in segregation of cognate genome element. The slow growth of Δ*parB1* mutant under normal as well as gamma stressed conditions as reported earlier (Charaka and Misra, 2012) further ascertained the indispensability of primary chromosome even in this multipartite genome harbouring bacterium.

The effect of parB deletions (making a phenotype of genome segregation defect) on gamma radiation dose response was checked in all the *parB* mutants. For that all the three mutants were maintained in the presence or absence of antibiotics selection pressure and their survival was monitored at different doses of gamma radiation, again in the presence or absence of antibiotics. Interestingly, *parB* mutants maintained without selection pressure but scored in the presence of antibiotics, showed higher sensitivity to gamma radiation as compared to the respective controls maintained under selection pressure (Fig. 7 A,C). This difference in gamma radiation response was not observed in case of Δ*parB2* and Δ*parB3* mutants when maintained under selection pressure and scored in the presence of antibiotics (Fig. 7B, D). Thus, the cells containing respective genome elements (scored as antibiotic resistance) did not lose resistance to gamma radiation, which implicate the role of these genome elements in radioresistance. These results suggested that ParB deletion can make cells defective in DNA segregation and loss of secondary genome elements, which can affect gamma radiation resistance without affecting their normal growth while defect in primary chromosome can affect both normal growth and eventually radiation stress tolerance.

4. Discussion

D. radiodurans, an extremotolerant bacterium, characterized for its extraordinary resistance to radiations and other DNA damaging agents (Slade and Radman, 2011). This bacterium also has an interesting cytogenetic feature like a multipartite genome system comprised of 2 chromosomes, megaplasmid and small plasmid, and each of these elements are present in multiple copies presumably packaged together in form of a toroidal nucleoid (White et al., 1999; Minsky et al., 2006). Functional significance of multiple chromosomes and ploidy in extreme phenotypes, and the mechanisms underlying faithful inheritance of multipartite genome system packaged in form of a compact toroidal nucleoid, into daughter cells are not known and offered the most interesting aspects in bacterial genome biology to investigate. Studies on genome partitioning in MGS system is limited to *V. cholera*e and *B. cenocepacica*, where each replicon (either chromosome or plasmids) have their own independent partitioning components responsible for their maintenance (Egan and Waldor, 2003; Egan et al., 2005; Dubarry et al., 2006). In case of *D. radiodurans* another multipartite genome harbouring bacterium, the partitioning system encoded on primary chromosome has been characterized and shown expressing characteristics of pulling mechanism of genome segregation (Charaka and Misra, 2012). Here, we have brought forth some evidence to highlight the role of ParBs encoded on chromosome II (ParB2) and megaplasmid (ParB3) in maintenance of cognate elements and their roles in the survival of *D. radiodurans* under both normal and stressed conditions. We found the homotypic interactions of all the ParBs while these ParBs do not interact to its other homologs in *D. radiodurans*. These results were expected because all ParBs have C-terminal domain, which is similar to ParBs of *T. thermophilus* and *P. aeruginosa* where the roles of C-terminal domain in dimerization of ParB proteins have been demonstrated (Leonard et al., 2004; Bartosik et al., 2004). Further ParBs are known as sequence specific centromere binding proteins that bind to centromere in dimeric form (Funnell, 2016) indicating that ParBs in this bacterium are most likely to be functional. This observation was further supported by *in vivo* protein-protein interaction using co-immunoprecipitation study from *D. radiodurans* expressing deinococcal ParBs fused at their N-terminal with different tags, on two plasmids (Fig. 3A–C). Earlier, we had reported that deletion of *parB1* in *D. radiodurans* imposes slower growth and segregation defects in primary chromosome (Charaka and Misra, 2012). In this study, when we compared the survival of Δ*parB2* and Δ*parB3* under normal and gamma stressed conditions with Δ*parB1* cells, we found that deletion of secondary genome ParBs has a little effect on normal growth as compared to wild type cells. The deletion of *parB1* presumably has arrested the segregation of chromosome I, which is not complemented by the presence of secondary genome ParBs (Fig. 6). This suggests that primary chromosome and secondary genome elements are most likely being maintained independently in this bacterium. Deletion of chromosomal ParB like proteins in *B. subtilis* and *P. aeruginosa* has affected genome segregation and normal growth in these bacteria (Ireton et al., 1994; Bartosik et al., 2004). An increase in copy number of replicons in respective *parB* mutants is intriguing and could not be explained with direct evidence. However, a strong interaction of replication initiation proteins like DnaA and DnaB, with all the ParB proteins of this bacterium allowed us to speculate on the cross talk of genome segregation and DNA replication. Similar findings have been

reported earlier in *V. cholerae* as well as in *B. subtilis* (Kadoya et al., 2011; Lee et al., 2003, 2006; Murray and Errington, 2008). The replicated origins occupying characteristic positions on genome have been shown in many bacteria. For instance, the replicated origins occupy at cell poles in *Caulobacter crescentus* (Mohl and Gober, 1997; Figge et al., 2003), at cell quarters in *Bacillus subtilis* (Lin et al., 1997; Webb et al., 1997, 1998; Sharpe and Errington, 1998) and near cell quarters or poles in *Escherichia coli* and *V. cholerae* (Gordon et al., 1997; Niki et al., 2000; Li et al., 2002; Lau et al., 2003; Figge et al., 2003; Egan and Waldor, 2003). Earlier it has been shown that ParABS system regulates the separation and maintenance of origin of replication (containing ParB binding sites near to it) at a characteristic subcellular position in the cells in *Bacillus subtilis*, *Caulobacter crescentus* and *Streptomyces coelicolor* A3 bacteria (Mohl and Gober, 1997; Lin and Grossman, 1998; Kim et al., 2000). These findings strongly support the interdependent regulation of DNA replication and genome partitioning in bacteria and provide the most plausible explanation for the effect of segregation defects on copy number of genome elements.

In conclusion, we report the functional characterization of ParBs encoded on multipartite genome system in *D. radiodurans* both *in vitro* and *in vivo*. ParB roles in regulation of genome copy number in multiparitte genome harboring bacteria is first time reported in any multipartite genome harboring bacteria. The molecular basis of *ori* regulation by ParBs and real time interaction of DNA replication machinery with multipartite genome segregation components would be the exciting area of bacterial genome biology and would be worth addressing independently. The available results together suggest that all ParBs exist as dimers, regulate genome segregation, and components of both genome segregation and DNA replication seem to interact with each other in this bacterium.

Conflict of interest

The authors declare that they have no conflicts of interest with the content of this article.

Acknowledgments

We thank Dr. Ajay Saini and Ms. Reema Singh for help in q-PCR experiments. GKM is grateful to the Department of Atomic Energy, Government of India for research fellowships.

Appendix A. Supplementary data

Supplementary material related to this article can be found, in the online version, at doi:https://doi.org/10.1016/j.micres.2019.03.005.

References

Bartosik, A.A., Lasocki, K., Mierzejewska, J., Thomas, C.M., Jagura-Burdzy, G., 2004. ParB of *Pseudomonas aeruginosa*: interactions with its partner ParA and its target *parS* and specific effects on bacterial growth. J. Bacteriol. 186 (20), 6983–6998.

Battesti, A., Bouveret, E., 2012. The bacterial two-hybrid system based on adenylate cyclase reconstitution in Escherichia coli. Methods 58, 325–334.

Battista, J.R., 2000. Radiation resistance: the fragments that remain. Curr. Biol. 10, R204–R205.

Battista, J.R., Park, M.J., McLemore, A.E., 2001. Inactivation of two homologues of proteins presumed to be involved in the desiccation tolerance of plants sensitizes *Deinococcus radiodurans* R1 to desiccation. Cryobiology 43, 133–139.

Breuert, S., Allers, T., Spohn, G., Soppa, J., 2006. Regulated polyploidy in halophilic archaea. PLoS One 1, e92.

Bustin, S.A., Benes, V., Garson, J.A., Hellemans, J., Huggett, J., Kubista, M., Mueller, R., Nolan, T., Pfaffl, M.W., Shipley, G.L., Vandesompele, J., 2009. The MIQE guidelines: minimum information for publication of quantitative real-time PCR. Clin. Chem. 55, 611–622.

Charaka, V.K., Misra, H.S., 2012. Functional characterization of the role of the chromosome I partitioning system in genome segregation in *Deinococcus radiodurans*. J. Bacteriol. 194, 5739–5748.

Charaka, V.K., Mehta, K.P., Misra, H.S., 2013. ParA encoded on chromosome II of *Deinococcus radiodurans* binds to nucleoid and inhibits cell division in *Escherichia coli*. J. Biosci. 38, 487–497.

Das, A.D., Misra, H.S., 2011. Characterization of DRA0282 from *Deinococcus radiodurans* for its role in bacterial resistance to DNA damage. Microbiology 157, 2196–2205.

Dubarry, N., Pasta, F., Lane, D., 2006. ParABS systems of the four replicons of *Burkholderia cenocepacia*: new chromosome centromeres confer partition specificity. J. Bacteriol. 188, 1489–1496.

Egan, E.S., Waldor, M.K., 2003. Distinct replication requirements for the two *Vibrio cholerae* chromosomes. Cell 114 (4), 521–530.

Egan, E.S., Fogel, M.A., Waldor, M.K., 2005. Divided genomes: negotiating the cell cycle in prokaryotes with multiple chromosomes. Mol. Microbiol. 56, 1129–1138.

Figge, R.M., Easter, J., Gober, J.W., 2003. Productive interaction between the chromosome partitioning proteins, ParA and ParB, is required for the progression of the cell cycle in Caulobacter crescentus. Mol. Microbiol. 47, 1225–1237.

Fogel, M.A., Waldor, M.K., 2005. Distinct segregation dynamics of the two *Vibrio cholerae* chromosomes. Mol. Microbiol. 55, 125–136.

Funnell, B.E., 2016. ParB partition proteins: complex formation and spreading at bacterial and plasmid centromeres. Front. Mol. Biosci. 3, 44.

Gerdes, K., Howard, M., Szardenings, F., 2010. Pushing and pulling in prokaryotic DNA segregation. Cell 141, 927–942.

Gordon, G.S., Sitnikov, D., Webb, C.D., Teleman, A., Straight, A., Losick, R., et al., 1997. Chromosome and low copy plasmid segregation in *E. coli*: visual evidence for distinct mechanisms. Cell 90, 1113–1121.

Green, M.R., Sambrook, J., 2012. Molecular Cloning: A Laboratory Manual. Cold Spring Harbor Laboratory Press, Cold Spring Harbor N.Y.

Hansen, M.T., 1978. Multiplicity of genome equivalents in the radiation-resistant bacterium Micrococcus radiodurans. J. Bacteriol. 134 (1), 71–75.

Harsojo, K.S., Matsuyama, A., 1981. Genome multiplicity and radiation resistance in Micrococcus radiodurans. J. Biochem. 90, 877–880.

Hayes, F., Barillà, D., 2006. The bacterial segrosome: a dynamic nucleoprotein machine for DNA trafficking and segregation. Nat. Rev. Microbiol. 4 (2), 133.

Ireton, K., Gunther, N.W., Grossman, A.D., 1994. spo0J is required for normal chromosome segregation as well as the initiation of sporulation in Bacillus subtilis. J. Bacteriol. 176 (17), 5320–5329.

Kadoya, R., Baek, J.H., Sarker, A., Chattoraj, D.K., 2011. Participation of chromosome segregation protein ParAI of Vibrio cholerae in chromosome replication. J. Bacteriol. 193 (7), 1504–1514.

Karimova, G., Pidoux, J., Ullmann, A., Ladant, D., 1998. A bacterial two-hybrid system based on a reconstituted signal transduction pathway. Proc. Nat. Acad. Sci. U. S. A. 95, 5752–5756.

Khairnar, N.P., Kamble, V.A., Misra, H.S., 2008. RecBC enzyme overproduction affects UV and gamma radiation survival of Deinococcus radiodurans. DNA Repair 7, 40–47.

Kim, H.J., Calcutt, M.J., Schmidt, F.J., Chater, K.F., 2000. Partitioning of the linear chromosome during sporulation of *Streptomyces coelicolor* A3 (2) involves an oriC-linked parAB locus. J. Bacteriol. 182 (5), 1313–1320.

Lau, I.F., Filipe, S.R., Soballe, B., Okstad, O.A., Barre, F.X., Sherratt, D.J., 2003. Spatial and temporal organization of replicating *Escherichia coli* chromosomes. Mol. Microbiol. 49, 731–743.

Lee, P.S., Grossman, A.D., 2006. The chromosome partitioning proteins Soj (ParA) and Spo0J (ParB) contribute to accurate chromosome partitioning, separation of replicated sister origins, and regulation of replication initiation in Bacillus subtilis. Mol. Microbiol. 60 (4), 853–869.

Lee, P.S., Lin, D.C.H., Moriya, S., Grossman, A.D., 2003. Effects of the chromosome partitioning protein Spo0J (ParB) on oriC positioning and replication initiation in Bacillus subtilis. J. Bacteriol. 185 (4), 1326–1337.

Leonard, T.A., Butler, P.J.G., Löwe, J., 2004. Structural analysis of the chromosome segregation protein Spo0J from Thermus thermophilus. Mol. Microbiol. 53 (2), 419–432.

Lewis, R.A., Bignell, C.R., Zeng, W., Jones, A.C., Thomas, C.M., 2002. Chromosome loss from par mutants of *Pseudomonas putida* depends on growth medium and phase of growth. Microbiology 148 (2), 537–548.

Li, Y., Sergueev, K., Austin, S., 2002. The segregation of the *Escherichia coli* origin and terminus of replication. Mol. Microbiol. 46, 985–996.

Lin, D.C.H., Grossman, A.D., 1998. Identification and characterization of a bacterial chromosome partitioning site. Cell 92, 675–685.

Lin, D.C.H., Levin, P.A., Grossman, A.D., 1997. Bipolar localization of a chromosome partition protein in Bacillus subtilis. Proc. Natl. Acad. Sci. U. S. A. 94, 4721–4726.

Maurya, G.K., Modi, K., Misra, H.S., 2016. Divisome and segrosome components of *Deinococcus radiodurans* interact through cell division regulatory proteins. Microbiology (UK) 162, 1321–1334.

Maurya, G.K., Modi, K., Banerjee, M., Chaudhary, R., Rajpurohit, Y.S., Misra, H.S., 2018. Phosphorylation of FtsZ and FtsA by a DNA damage-responsive Ser/Thr protein kinase affects their functional interactions in *Deinococcus radiodurans*. mSphere 3 (4).

Minsky, A., Shimoni, E., Englander, J., 2006. Ring-like nucleoids and DNA repair through error-free nonhomologous end joining in *Deinococcus radiodurans*. J. Bacteriol. 188 (17), 6047–6051.

Misra, H.S., Khairnar, N.P., Kota, S., Srivastava, S., Joshi, V.P., Apte, S.K., 2006. An exonuclease I sensitive DNA repair pathways in *Deinococcus radiodurans*: a major determinant of radiation resistance. Mol. Microbiol. 59, 1308–1316.

Misra, H.S., Rajpurohit, Y.S., Kota, S., 2013. Physiological and molecular basis of extreme radioresistance in Deinococcus radiodurans. Curr. Sci. 104, 194–206.

Misra, H.S., Maurya, G.K., Kota, S., Charaka, V.K., 2018. Maintenance of multipartite genome system and its functional significance in bacteria. J. Genet. 97 (4), 1013–1038.

Mohl, D.A., Gober, J.W., 1997. Cell cycle–dependent polar localization of chromosome partitioning proteins in *Caulobacter crescentus*. Cell 88 (5), 675–684.

Murray, H., Errington, J., 2008. Dynamic control of the DNA replication initiation protein DnaA by Soj/ParA. Cell 135 (1), 74–84.

Niki, H., Yamaichi, Y., Hiraga, S., 2000. Dynamic organization of chromosomal DNA in *Escherichia coli*. Genes Dev. 14, 212–223.
Saint-Dic, D., Frushour, B.P., Kehrl, J.H., Kahng, L.S., 2006. A parA homolog selectively influences positioning of the large chromosome origin in Vibrio cholerae. J. Bacteriol. 188 (15), 5626–5631.
Schaefer, M.C., Schmitz, R., Facius, G., Horneck, B., Milow, K.H., Ortner, J., 2000. Systematic study of parameters influencing the action of Rose Bengal with visible light on bacterial cells: comparison between biological effect and singlet-oxygen production. Photochem. Photobiol. 71, 514–523.
Sharpe, M.E., Errington, J., 1998. A fixed distance for separation of newly replicated copies of *oriC* in *Bacillus subtilis*: implications for co-ordination of chromosome segregation and cell division. Mol. Microbiol. 28, 981–990.
Slade, D., Radman, M., 2011. Oxidative stress resistance in Deinococcus radiodurans. Microbiol. Mol. Biol. Rev. 75, 133–191.
Webb, C.D., Teleman, A., Gordon, S., Straight, A., Belmont, A., Lin, D.C.H., et al., 1997. Bipolar localization of the replication origin regions of chromosomes in vegetative and sporulating cells of *B. subtilis*. Cell 88, 667–674.
Webb, C.D., Graumann, P.L., Kahana, J.A., Teleman, A.A., Silver, P.A., Losick, R., 1998. Use of time-lapse microscopy to visualize rapid movement of the replication origin region of the chromosome during the cell cycle in *Bacillus subtilis*. Mol. Micribiol. 28, 883–892.
White, O., Eisen, J.A., Heidelberg, J.F., Hickey, E.K., Peterson, J.D., Dodson, R.J., et al., 1999. Genome sequence of the radioresistant bacterium *Deinococcus radiodurans* R1. Science 286, 1571–1577.
Yanagida, M., 2005. Basic mechanism of eukaryotic chromosome segregation. Philos. Trans. R. Soc. Lond. B Biol. Sci. 360, 609–621.